# Ligand Influences on Copper Cyanide Solid-State Architecture: Flattened and Fused "Slinky", Corrugated Sheet, and Ribbon Motifs in the Copper−Cyanide−Triazolate−Organoamine Family

**Douglas J. Chesnut, Anakarin Kusnetzow, Robert Birge, and Jon Zubieta***

Department of Chemistry, Room 1-014, Center for Science and Technology, and
W. M. Keck Center for Molecular Electronics, Syracuse University, Syracuse, New York 13244-4100

*Received April 7, 1999*

A series of novel composite inorganic−organic materials from the copper−cyanide−triazolate−organoamine system have been isolated and structurally characterized. An unusual interpenetrating layered structure type composed of fused and flattened "slinkies", $[Cu_6(CN)_5(trz)]$ (**1**) (trz = triazolate, $C_2N_3H_2^-$), a complex corrugated layer structure, $[Cu_5(CN)_3(trz)_2(bpy)]$ (**2**), and a series of increasingly intricate one-dimensional ribbons, $[Cu_3(CN)_2(trz)(bpy)]$, $[Cu_3(CN)_2(trz)(phen)]$, and $[Cu_4(CN)_3(trz)(phen)]$ (**3**−**5**), have been isolated from hydrothermal media. All trz ligands are deprotonated and participate in $\mu_3$-bridging of Cu sites. An anionic layered compound, $[Cu(OH_2)_4][Cu_4(CN)_6]$ (**6**), composed of $\{Cu_6(CN)_6\}$ rings with tetraaquacupric dications intercalated into alternate interlamellar spaces, has also been characterized upon the slow evaporation of the mother liquor of **1**. The syntheses and structural characterizations of compounds **1**−**6** by single-crystal X-ray diffraction and FTIR microscopy are discussed in relation to the supramolecular chemistry of other copper cyanide solid-state materials. Crystal data: $C_7H_2Cu_6N_8$ (**1**), orthorhombic, *Pcca*, $a = 11.108(2)$ Å, $b = 8.886(2)$ Å, $c = 15.397(3)$ Å, $Z = 4$; $C_{34}H_{24}Cu_{10}N_{22}$ (**2**), triclinic, $P\bar{1}$, $a = 9.1183(5)$ Å, $b = 9.9838(6)$ Å, $c = 12.7545(8)$ Å, $\alpha = 94.206(1)°$, $\beta = 90.492(1)°$, $\gamma = 112.534(1)°$, $Z = 1$; $C_{28}H_{20}Cu_6N_{14}$ (**3**), monoclinic, $P2_1/c$, $a = 9.7582(1)$ Å, $b = 17.1622(2)$ Å, $c = 9.901(1)$ Å, $\beta = 106.869(1)°$, $Z = 2$; $C_{17}H_{10}Cu_4N_8$ (**4**), monoclinic, $P2_1/c$, $a = 11.590(3)$ Å, $b = 20.555(4)$ Å, $c = 16.158(3)$ Å, $\beta = 103.865(5)°$, $Z = 8$; $C_{16}H_{10}Cu_3N_7$ (**5**), triclinic, $P\bar{1}$, $a = 8.542(2)$ Å, $b = 9.802(2)$ Å, $c = 20.439(4)$ Å, $\alpha = 82.468(5)°$, $\beta = 83.126(5)°$, $\gamma = 79.832(5)°$, $Z = 4$; $C_6Cu_5N_6O_4$ (**6**), monoclinic, $P2_1/n$, $a = 7.466(1)$ Å, $b = 8.952(2)$ Å, $c = 11.116(2)$ Å, $\beta = 92.816(5)°$, $Z = 4$.

## Introduction

The driving force for the development of new materials derives from their potential applications to fields as diverse as catalysis, sorption, and molecular electronics.[1] It is highly desirable to be able to alter the microstructures of solid-state materials so as to tune their physicochemical properties.[2] Exploitation of organic components which introduce specific geometric requirements has been proposed as one strategy for the controlled manipulation of the microstructures of novel solid-state materials.[3,4] Incorporation of organic components into inorganic−organic solid-state composite materials with hierarchical structures of increasing complexity has been demonstrated in materials such as zeolites,[5] MCM-41 mesoporous oxides,[6] transition metal phosphates templated with organic components,[7] and Nature's remarkable products of biomineralization.[8] The incorporation of ligands LL (where LL is an aromatic and chelating nitrogen donor ligand) into hybrid materials as templating, space-filling, and passivating agents has provided an increasingly successful preparative strategy.

Traditional high-temperature methods for preparing inorganic solid-state materials generally lead to the isolation of thermodynamic phases. To modify the microstructures of solid-state materials, a shift to the kinetic domain is required to provide access to metastable phases.[9] A variety of chimie douce methods have been developed and applied to the isolation of such metastable phases, which are often inaccessible by more traditional methods.[10]

Of these chimie douce, or soft chemical, methods, reactions occurring in hydrothermal media are yielding a rich array of chemical products for a variety of systems.[11] The complexity of the hydrothermal reaction domain often allows subtle changes in reaction conditions to provide unique solid-state structures. For a given chemical system, these structures are often constructed from the same or relatively similar achitectural motifs.[12]

Transition metal cyanide systems have been extensively investigated for their rich supramolecular chemistry and poten-

* To whom correspondence should be addressed at the Department of Chemistry.

(1) Cheetham, A. K. *Science* **1994**, *264*, 794.
(2) Stupp, S. I.; Braun, P. V. *Science* **1997**, *277*, 1242.
(3) Mann, S.; Ozin, G. A. *Nature* (*London*) **1996**, *382*, 313.
(4) Mann, S. *J. Chem. Soc., Dalton Trans.* **1997**, 3953.
(5) (a) Smith, J. V. *Chem. Rev.* **1988**, *88*, 149. (b) Occelli, M. L.; Robson, H. C. *Zeolite Synthesis*; American Chemical Society: Washington, DC, 1989.
(6) Kresge, C. T.; Leonowicz, M. E.; Roth, W. J.; Vartuli, J. C.; Beck, J. S. *Nature* (*London*) **1992**, *359*, 710.
(7) (a) Haushalter, R. C.; Mundi, L. A. *Chem. Mater.* **1992**, *4*, 31. (b) Khan, M. I.; Meyer, L. M.; Haushalter, R. C.; Schmeitzer, C. L.; Zubieta, J.; Dye, J. L. *Chem. Mater.* **1996**, *8*, 43.
(8) Mann, S. *Nature* **1993**, *365*, 499.
(9) Gopalakrishnan, J. *Chem. Mater.* **1995**, *7*, 1265.
(10) Stein, A.; Keller, S. W.; Mallouk, T. E. *Science* **1993**, *257*, 1558.
(11) Chesnut, D. J.; Hagrman, D.; Zapf, P. J.; Hammond, R. P.; LaDuca, R., Jr.; Haushalter, R. C.; Zubieta, J. *Coord. Chem. Rev.*, in press.
(12) Hagrman, D.; Zapf, P. J.; Zubieta, J. *Angew. Chem., Int. Ed. Engl.*, in press.

10.1021/ic990385q CCC: $18.00 
Published on Web 11/06/1999

tially interesting magnetic properties, both of which emanate from the effectiveness of the cyanide unit as a bridging ligand.[13] The organoamine 1,2,4-triazole is also often employed to fulfill the bridging function between metal centers for similar purposes.[14] However, the structural versatility of triazolate as a tripodal linker between metal centers in solid-state compounds had not been fully realized until hydrothermal conditions were exploited to minimize differential solubilities and to effect crystallization.[15]

The copper cyanide system is particularly attractive from the viewpoint of structural engineering because of the previously reported versatility of $\{Cu_x(CN)_y\}_n$ structural motifs in accommodating various ligand-imposed geometric requirements.[16−19] The triazolate group likewise serves as an effective bridging ligand between metal centers and allows propagation of structural information in two dimensions. Thus, the flexible chain $\{Cu_x(CN)_y\}_\infty$ unit and the rigid tripodal triazolate motif provide simple components for a building block approach to solid-state materials. Furthermore, the triazolate ligand may stabilize Cu(II) sites and allow the isolation of mixed-valence Cu(I)/Cu(II) materials from hydrothermal media so as to provide materials with magnetic properties.

The structural chemistry of the Cu−CN−triazolate family may also be manipulated through the expedient of introducing chelating ligands LL which perform in templating, space-filling, or passivating roles. Specifically, sterically demanding, chelating groups can function as capping ligands, effectively restricting the spatial extension of the structure to one dimension.[20] From the prospective of assessing the effect of ligand geometries and coordination modes and of metal coordination preferences on the design of solid architectures, the Cu−CN−trz−organoamine system provides a readily accessible synthetic chemistry for the development of a structural database for a building block approach to solid-state materials.

In the course of this study, the compounds $[Cu_6(CN)_5(trz)]$ (**1**) (trz = 1,2,4-trizaolate, $C_2N_3H_2^-$), $[Cu_5(CN)_3(trz)_2(bpy)]$ (**2**) (bpy = 2,2′-bipyridyl), $[Cu_3(CN)_2(trz)(bpy)]$ (**3**), $[Cu_3(CN)_2(trz)(phen)]$ (**4**) (phen = 1,10-phenanthroline), $[Cu_4(CN)_3(trz)(phen)]$ (**5**), and $[Cu(OH_2)_4][Cu_4(CN)_6]$ (**6**) were isolated and structurally characterized. Here we report the syntheses and structural characterizations of novel interpenetrating layered structures composed of fused and flattened "slinkies" (**1**), an unusual corrugated layered structure (**2**), a pair of ribbon structures based on similar motifs (**3** and **4**), a unique ribbon structure with a "stair-step" core (**5**), and an anionic layered structure of $\{Cu_6(CN)_6\}_\infty$ rings with tetraaquacupric dications intercalated into the interlamellar regions (**6**).

## Experimental Section

**Syntheses.** All reagents were obtained from Aldrich and used as received without further purification. *Caution* should be exercised when handling cyanide salts due to their toxicity and the potential for generating HCN should such salts come into contact with acids. All compounds were prepared by the successive addition of the reagents to 0.5 in. i.d. heavy wall borosilicate tubes of ca. 10 in. length. The tubes were subsequently sealed. The final charge volume of the tubes was ca. 65%. The tubes were then placed in an oven for 140.3 h at 180 ± 5 °C. The duration of the heating cycle was determined by visual inspection of the vessels. Some crystalline products were observed after ca. 4 h. The vessels were then removed from the oven. The tubes were subsequently opened with the exception of the vessel from which **1** and **6** were isolated, which remained sealed for approximately 2 weeks.

**Chart 1**

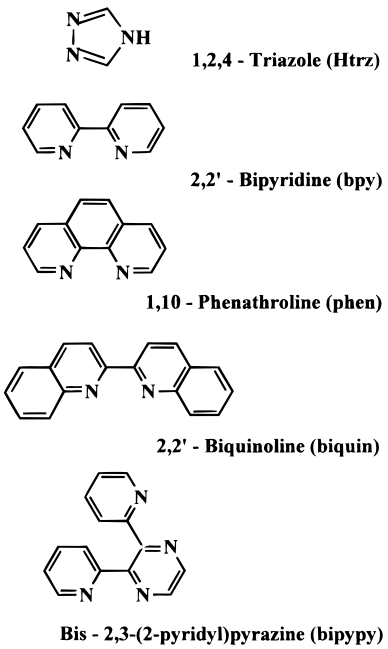


**$[Cu_6(CN)_5(trz)]$ (1).** $[Cu_6(CN)_5(trz)]$ was prepared as clear yellow-tinted crystalline rods by the successive addition of CuCN (0.364 g, 4.03 mmol), KCN (0.061 g, 0.94 mmol), 1,2,4-triazole (Htrz, Chart 1) (0.062 g, 0.92 mmol), and $H_2O$ (10.00 mL, 0.536 mol) to a reaction vessel. The reaction vessel was then sealed and subsequently placed in an oven for 140.3 h at 180 ± 5 °C.

Upon removal of the vessel from the oven at the end of the time indicated, the only crystalline phase observed by eye was composed of clear, pale-yellow-tinted crystals. The contents were transferred in toto to a Petrie dish with 5 mL of deionized wash water and inspected using a microscope equipped with a 4× objective lens. A single crystal of dimensions 0.40 × 0.35 × 0.05 mm was selected.

A small amount of green amorphous solid proved uncharacterizable via single-crystal X-ray diffraction and was not examined further. The mother liquor was covered and left to stand for a period of several weeks. Upon evaporation, thin purple plates of **6** were isolated in low yield.

**$[Cu_5(CN)_3(trz)_2(bpy)]$ (2) and $[Cu_3(CN)_2(trz)(bpy)]$ (3).** Compounds **2** and **3** were prepared as clear red crystals of distorted cubic habit and clear yellow-orange crystals, respectively, by the successive addition of CuCN (0.360 g, 4.02 mmol), KCN (0.061 g, 0.94 mmol), Htrz (0.069 g, 1.0 mmol), 2,2′-bipyridyl (bpy, Chart 1) (0.154 g, 0.986 mmol), and $H_2O$ (10.00 mL, 0.536 mol) to the reaction vessel described. The reaction vessel was then sealed and subsequently placed in an oven for 140.3 h at 180 ± 5 °C.

The reaction vessel contained a clear and colorless solution, masses of canary yellow, granular particles; nearly opaque, massive cherry red rhomboidal crystals; smaller red crystals of distorted cubic habit, and clear yellow orange crystals. After allowing the vessel to stand for ca. 4 h, the vessel was opened, and the solid contents were then collected using standard vacuum filtration techniques. The mother liquor was discarded.

(13) Iwamoto, T. In *Comphrehensive Supramolecular Chemistry*; Atwood, J. L., Davies, J. E. D., MacNicol, D. D., Eds.; Pergamon: New York, 1996; Vol. 6, p 643.
(14) Garcia, Y.; von Koningsbruggen, P. J.; Bravic, G.; Guionneau, P.; Chasseau, D.; Cascarano, G. L.; Moscvici, J.; Lambert, K.; Michalowicz, A.; Kahn, O. *Inorg. Chem.* **1997**, *36*, 6357 and refs 1−22 therein.
(15) Hagrman, D.; Zubieta, J. *J. Chem. Soc., Chem. Commun.* **1998**, 2005.
(16) Chesnut, D. J.; Zubieta, J. *J. Chem. Soc., Chem. Commun.* **1998**, 1707.
(17) Chesnut, D. J.; A. Kusnetzow, A.; Zubieta, J. *J. Chem. Soc., Dalton Trans.* **1998**, 4081.
(18) Chesnut, D. J.; Kusnetzow, A.; Birge, B. W.; Zubieta, J. A. *Inorg. Chem.* **1999**, *38*, 2663.
(19) Stocker, F. B.; Staeva, T. P.; Rienstra, C. M.; Britton, D. *Inorg. Chem.* **1999**, *38*, 984.
(20) Zapf, P. J.; Hammond, R. P.; Haushalter, R. C.; Zubieta, J. *Chem. Mater.* **1998**, *10*, 1366.

**Table 1.** Crystallographic Data for Compounds **1**−**6**

| | **1** | **2** | **3** | **4** | **5** | **6** |
|---|---|---|---|---|---|---|
| empirical formula | $C_7H_2Cu_6N_8$ | $C_{34}H_{24}Cu_{10}N_{22}$ | $C_{28}H_{20}Cu_6N_{14}$ | $C_{16}H_{10}Cu_3N_7$ | $C_{17}H_{10}Cu_4N_8$ | $C_6H_8Cu_5N_6O_4$ |
| fw | 579.4 | 1376.15 | 933.82 | 490.93 | 580.49 | 545.88 |
| space group (No.) | *Pcca* (54) | $P\bar{1}$ (2) | $P2_1/c$ (14) | $P\bar{1}$ (2) | $P2_1/c$ (14) | $P2_1/n$ (14) |
| *a* (Å) | 11.108(2) | 9.1183(5) | 9.7582(1) | 8.542(2) | 11.590(3) | 7.466(1) |
| *b* (Å) | 8.886(2) | 9.9838(6) | 17.1622(2) | 9.802(2) | 20.555(4) | 8.952(2) |
| *c* (Å) | 15.397(3) | 12.7545(8) | 9.901(1) | 20.439(4) | 16.158(3) | 11.116(2) |
| α (deg) | 90 | 94.206(1) | 90 | 82.468(5) | 90 | 90 |
| *β* (deg) | 90 | 90.492(1) | 106.869(1) | 83.126(5) | 103.865(5) | 92.816(5) |
| *γ* (deg) | 90 | 112.534(1) | 90 | 79.832(5) | 90 | 90 |
| *V* (Å$^3$), *Z* | 1519.8(5), 4 | 1068.7(1), 1 | 1586.86(2), 2 | 1661.7(6), 4 | 3737(1), 8 | 742.0(3), 2 |
| *T* (K) | 115 | 115 | 115 | 115 | 115 | 115 |
| *λ* (Å) | 0.710 73 | 0.710 73 | 0.710 73 | 0.710 73 | 0.710 73 | 0.710 73 |
| $\rho_{calcd}$ (g cm$^{-3}$) | 2.532 | 2.138 | 1.954 | 1.962 | 2.063 | 2.443 |
| *μ* (mm$^{-1}$) | 8.243 | 4.925 | 3.994 | 3.819 | 4.512 | 7.067 |
| $R$,[a] $R_w$[b] (%) | 2.40, 6.08 | 4.19, 10.38 | 2.65, 5.74 | 4.21, 10.52 | 3.27, 7.92 | 4.42, 9.68 |

[a] $R = \sum||F_o| - |F_c||/\sum|F_o|$. [b] $R_w = [\sum[w(F_o^2 - F_c^2)^2]/\sum[w(FF_o^2)^2]]^{1/2}$.

**Table 2.** Selected Bond Lengths (Å) and Angles (deg) for Compound **1**[a]

| | | | | | |
|---|---|---|---|---|---|
| Cu1−X2 | 1.829(2) | Cu1−X1 | 1.837(2) | Cu2−X3 | 1.891(2) |
| Cu2−N6 | 1.993(3) | Cu3−N7 | 1.891(2) | Cu3−X4 | 1.853(2) |
| Cu4−X5 | 1.836(2) | X1−X1A | 1.153(5) | X2−X3 | 1.160(3) |
| X4−X5 | 1.152(3) | | | | |

| | | | |
|---|---|---|---|
| X1−Cu1−X2 | 174.5(1) | X3A−Cu2−N6 | 109.08(7) |
| X3−Cu2−N6 | 109.08(7) | X3A−Cu2−X3 | 141.8(1) |
| X4−Cu3−N7 | 168.3(1) | X5A−Cu5−X5 | 180.0(1) |

[a] X = a disordered cyanide member atom position.

**Table 3.** Selected Bond Lengths (Å) and Angles (deg) for Compound **2**[a]

| | | | | | |
|---|---|---|---|---|---|
| Cu1−X1 | 1.839(4) | Cu2−X2 | 1.817(4) | Cu2−X3 | 1.939(4) |
| Cu2−N7 | 1.989(4) | Cu3−X4 | 1.879(5) | Cu3−N8 | 1.990(4) |
| Cu3−N10 | 1.997(3) | Cu4−X5 | 1.893(4) | Cu4−N9 | 1.995(3) |
| Cu4−N11 | 1.960(3) | Cu5−N12 | 1.897(3) | Cu6−X6 | 1.865(4) |
| Cu6−N13 | 2.077(4) | Cu6−N14 | 2.012(4) | X1−X2 | 1.147(6) |
| X3−X4A | 1.157(6) | X5−X6 | 1.159(6) | | |

| | | | |
|---|---|---|---|
| X1−Cu1−X1A | 180.000(1) | X2−Cu2−X3 | 129.1(1) |
| X2−Cu2−N7 | 127.7(1) | X3−Cu2−N7 | 102.7(1) |
| X4−Cu3−N8 | 124.3(1) | X4−Cu3−N10 | 127.2(1) |
| N8−Cu3−N10 | 108.4(1) | X5−Cu4−N9 | 112.8(1) |
| X5−Cu4−N11 | 136.6(1) | N12−Cu5−N12A | 180.000(1) |
| N9−Cu4−N11 | 110.2(1) | X6−Cu6−N13) | 124.9(1) |
| X6−Cu6−N14 | 151.0(3) | N13−Cu6−N14 | 80.7(1) |

[a] X = a disordered cyanide member atom position.

Characterization by X-ray crystallography of the granular, canary yellow solids was not attempted due to poor crystallinity as determined by visual inspection. The massive rhomboidal red crystals were determined to be the previously reported $[(bpy)Cu)_2(CN)]_2[Cu_5(CN)_7]\cdot {}^1/_6H_2O$.

A single red crystal of distorted cubic habit, **2**, with dimensions of 0.08 × 0.05 × 0.04 mm and a single crystal of the yellow orange phase, **3**, of dimensions 0.30 × 0.09 × 0.08 mm were chosen for use in single-crystal diffraction experiments.

Attempts at optimizing yields of **2** and **3** and at obtaining monophasic materials were unsuccessful.

**$[Cu_3(CN)_2(trz)(phen)]$ (4) and $[Cu_4(CN)_3(trz)(phen)]$ (5).** Compounds **4** and **5** were prepared by the successive addition of CuCN (0.357 g, 3.99 mmol), KCN (0.063 g, 0.97 mmol), Htrz (0.061 g, 0.88 mmol), 1,10-phenanthroline (phen, Chart 1) (0.178 g, 0.9886 mmol), and $H_2O$ (10.00 mL, 0.536 mol) to a reaction vessel. The reaction vessel was then sealed and subsequently placed in an oven for 140.3 h at 180 ± 5 °C. The reaction vessel was observed to contain a clear and colorless solution, granular canary yellow solids, an orange crystalline solid, and a yellow crystalline solid.

The vessel was allowed to cool for ca. 4 h prior to opening. The solid contents were collected using standard vacuum filtration techniques, and the mother liquor was discarded. Again, the granular canary yellow solid was not characterized. A single orange crystal of **4** of dimensions 0.60 × 0.60 × 0.05 mm and a single yellow crystal of **5** of dimensions 0.41 × 0.30 × 0.09 mm were chosen for use in single-crystal X-ray diffraction experiments.

**$[Cu(OH_2)_4]\{Cu_4(CN)_6\}$ (6).** Compound **6** was observed as thin, clear, pale purple plates which had coalesced around minute (diameter <0.005 mm) particles of the green amorphous phase described during the preparation of **1**. A crystal of the purple phase was selected for use in a single-crystal X-ray diffraction experiment by fracturing individual plates so as to avoid including the green phase in the final sample when it was viewed using a microscope equipped with a 6× objective lens. The final dimensions of the crystal were 0.05 × 0.05 × 0.01 mm.

**Reaction Chemistry of CuCN and Htrz with biquin and bipypy.** Reactions similar to those described were conducted using the organoamines biquin and bipypy (Chart 1) in combination with Htrz. The reaction products observed for the trial employing biquin were a clear and colorless solution over an intermixed mass of orange-yellow and red crystalline phases. The orange-yellow phase was determined to be $[Cu_2(CN)_2(biquin)]$, whose structure will be reported elsewhere. The red phase was determined to be the previously reported compound $[Cu_4(CN)_4(biquin)]$.[16] The products of the hydrothermal reaction of CuCN, KCN, and bipypy were a clear and colorless solution over wine-red crystalline panes. The wine-red solid phase was determined to be the recently reported interdigitating layered structure $[Cu_3(CN)_3(bipypy)]$.[18]

**X-ray Crystallographic Studies.** Structural studies of compounds **1**−**6** were performed on a Bruker SMART CCD diffractometer with graphite-monochromated Mo Kα radiation [$\lambda$(Mo Kα) = 0.710 73 Å]. The data were collected at 115 ± 3 K using slow *ω* scans with narrow frames. Crystallographic data for compounds **1**−**6** are listed in Table 1. Empirical absorption corrections were applied to all compounds using SADABS software.[21] The structures were solved by direct methods.[22] All non-hydrogen atoms were refined anisotropically. Hydrogen atoms were placed at idealized positions with the exception of protons of the waters of hydration of the tetraaquacupric dication of compound **6**. Neutral-atom scattering factors were taken from ref 23. All structure solution and refinement calculations were performed using the SHELXTL crystallographic software package.[24] All graphics were prepared using the SHELXTL and Crystalmaker software packages.[24,25]

(21) Sheldrick, G. M. *SADABS: Program for Empirical Absorption Corrections*; University of Göttingen: Göttingen, Germany, 1986.
(22) Sheldrick, G. M. *SHELXTL: Structure Determination Programs*, Version 5.0; PC Siemens Analytical X-ray Instruments: Madison, WI, 1994.
(23) Macgillary, C. H., Rieck, G. D., Eds. *International Tables for Crystallography*; Kynoch Press: Birmingham, England, 1962; Vol. III.
(24) Sheldrick, G. M. *SHELXTL: Structure Determination Programs*, Version 5.0; PC Siemens Analytical X-ray Instruments: Madison, WI, 1994.
(25) Palmer, D. C. *Crystalmaker*[2], Version 2.1.6; Apple Computer, Inc.: Oxfordshire, U.K.; 1994−1997.

**Table 4.** Selected Bond Lengths (Å) and Angles (deg) for Compound **3**[a]

| | | | | | |
|---|---|---|---|---|---|
| Cu1−X4 | 1.891(2) | Cu1−N5 | 1.945(1) | Cu1−N6 | 2.026(1) |
| Cu2−X1 | 1.916(2) | Cu2−X3 | 1.880(2) | Cu2−N7 | 2.047(2) |
| Cu3−X2 | 1.867(2) | Cu3−N8 | 2.024(2) | Cu3−N9 | 2.047(2) |
| X1−X2 | 1.154(3) | X3−X4 | 1.157(3) | | |

| | | | |
|---|---|---|---|
| X4−Cu1−N5 | 138.07(9) | X4−Cu1−N6 | 111.43(8) |
| N5−Cu1−N6 | 110.45(7) | X1−Cu2−X3 | 143.45(9) |
| X1−Cu2−N7 | 101.11(8) | X3−Cu2−N7 | 115.34(8) |
| N8−Cu3−N9 | 80.87(8) | X2−Cu3−N8 | 145.95(9) |
| X2−Cu3−N9 | 130.68(9) | | |

[a] X = a disordered cyanide member atom position.

**Table 5.** Selected Bond Lengths (Å) and Angles (deg) for Compound **4**[a]

| | | | | | |
|---|---|---|---|---|---|
| Cu1−X1 | 1.870(3) | Cu2−X2 | 1.875(3) | Cu2−X3 | 1.906(3) |
| Cu2−N9 | 2.027(3) | Cu3−X6 | 1.889(3) | Cu3−X7 | 1.909(3) |
| Cu3−N12 | 2.036(3) | Cu4−N14 | 1.943(3) | Cu4−X5A | 1.883(3) |
| Cu5−X4 | 1.852(4) | Cu5−N15 | 2.026(3) | Cu5−N16 | 2.058(3) |
| Cu6−X8 | 1.855(4) | Cu6−N17 | 2.067(3) | Cu6−N18 | 2.009(3) |
| X1−X2 | 1.158(5) | X3−X4 | 1.158(5) | X5−X6 | 1.143(5) |
| X7−X8 | 1.151(5) | | | | |

| | | | |
|---|---|---|---|
| X1−Cu1−N10A | 140.6(1) | X1−Cu1−N11A | 111.0(1) |
| N10−Cu1−N11 | 108.2(1) | X2−Cu2−X3 | 140.9(1) |
| X2−Cu2−N9 | 116.1(1) | X3−Cu2−N9 | 103.0(1) |
| X6−Cu3−X7 | 140.4(1) | X6−Cu3−N12 | 115.8(1) |
| X7−Cu3−N12 | 103.6(1) | N14−Cu4−N13A | 110.4(1) |
| N14−Cu4−X5A | 138.3(1) | X5A−Cu4−N13A | 111.3(1) |
| X4−Cu5−N15 | 139.1(1) | X4−Cu5−N16 | 137.9(1) |
| N15−Cu5−N16 | 82.1(1) | X8−Cu6−N17 | 133.0(1) |
| X8−Cu6−N18 | 144.1(1) | N17−Cu6−N18 | 82.2(1) |

[a] X = a disordered cyanide member atom position.

**Table 6.** Selected Bond Lengths (Å) and Angles (deg) for Compound **5**[a]

| | | | | | |
|---|---|---|---|---|---|
| Cu1−X2 | 1.866(3) | Cu1−N18 | 1.936(2) | Cu2−X3 | 1.858(3) |
| Cu2−N19 | 2.046(2) | Cu2−N20 | 2.046(2) | Cu3−X4 | 1.926(2) |
| Cu3−X5 | 1.875(3) | Cu3−N17 | 2.027(2) | Cu4−X6 | 1.935(2) |
| Cu4−X7 | 1.881(3) | Cu4−N15 | 2.023(2) | Cu5−X8 | 1.839(2) |
| Cu5−X9 | 1.839(2) | Cu6−X10 | 1.859(3) | Cu6−N21 | 2.013(2) |
| Cu6−N22 | 2.081(3) | Cu7−X11 | 1.841(2) | Cu7−N13 | 1.868(2) |
| Cu8−X12 | 1.884(3) | Cu8−X1A | 1.906(2) | Cu8−N14 | 2.011(2) |
| X1−X2 | 1.164(4) | X3−X4 | 1.160(4) | X5−X6 | 1.160(4) |
| X7−X8 | 1.162(4) | X9−X10 | 1.154(4) | X11−X12A | 1.151(4) |
| Cu1−N16A | 2.028(2) | | | | |

| | | | |
|---|---|---|---|
| X2−Cu1−N18 | 141.3(1) | X2−Cu1−N16A | 110.4(1) |
| N18−Cu1−N16A | 108.04(9) | X3−Cu2−N19 | 137.8(1) |
| X3−Cu2−N20 | 140.5(1) | N19−Cu2−N20 | 81.62(9) |
| X4−Cu3−X5 | 142.6(1) | X4−Cu3−N17 | 100.8(1) |
| X5−Cu3−N17 | 116.5(1) | X6−Cu4−X7 | 133.4(1) |
| X6−Cu4−N15 | 103.83(9) | X7−Cu4−N15 | 122.7(1) |
| X8−Cu5−X9 | 171.9(1) | X10−Cu6−N21 | 150.8(1) |
| X10−Cu6−N22 | 127.3(1) | N21−Cu6−N22 | 81.91(9) |
| X11−Cu7−N13 | 174.1(1) | X12−Cu8−X1A | 132.0(1) |
| X12−Cu8−N14 | 116.0(1) | N14−Cu8−X1A | 112.0(1) |

[a] X = a disordered cyanide member atom position.

The cyano groups of compounds **1**−**6** are disordered with respect to the C and N termini. This conclusion reflected the observation that wR2 minimized upon adopting 50% C and N occupancies at those sites. Consequently, the final site populations arrived at were 50% of each atom type per site X. Subsequent refinement of the temperature factors was unexceptional.

Significant bond lengths and angles of **1**−**6** are compiled in Tables 2−7.

**FTIR Spectroscopy.** Fourier transform infrared spectra of compounds **1**−**5** were obtained using a Nicolet Nic-Plan IR microscope coupled to a Nicolet Magna IR 750. Single crystals of the compounds were selected on the basis of thickness and lack of impurities, i.e., inclusions. A spectrum of compound **6** was not obtained due to microscopic inclusions of green solids which precluded obtaining a homogeneous sample region. Detector saturation over the cyanide stretching region was observed during the collection of the spectra for **2**−**5**. Saturation was not avoidable by reducing the sample thickness, as thinner crystals devoid of fractures were not observed at the 32× magnification of the experiment.

Crystals of compounds **1**−**5** were mounted on $CaF_2$ windows (4000−1100 $cm^{-1}$), and images were focused using a 32× IR objective lens. Transmission spectra were collected and averaged (516 scans at a resolution of 2 $cm^{-1}$); the area scanned was 10 $\mu$m in diameter. The detector used to collect the data was a liquid $N_2$ cooled MCT-A detector. The OMNIC 3.1 software package was used to collect and process all data.[26]

**Table 7.** Selected Bond Lengths (Å) and Angles (deg) for Compound **6**[a]

| | | | | | |
|---|---|---|---|---|---|
| Cu1−X1 | 1.907(6) | Cu1−X2 | 1.946(5) | Cu1−X3 | 1.974(5) |
| Cu2−X4 | 1.924(6) | Cu2−X5 | 1.905(5) | Cu2−X6 | 1.980(5) |
| Cu3−O1 | 2.043(4) | Cu3−O2 | 2.024(4) | X1−X6A | 1.155(7) |
| X2−X5A | 1.157(7) | X3−X4 | 1.150(7) | | |

| | | | |
|---|---|---|---|
| X1−Cu1−X2 | 130.8(2) | X2−Cu1−X3 | 106.4(2) |
| X3−Cu1−X1 | 122.7(2) | X4−Cu2−X5 | 132.5(2) |
| X5−Cu2−X6 | 120.4(2) | X6−Cu2−X4 | 107.0(2) |
| O1−Cu3−O2 | 88.8(2) | O1−Cu3−O1A | 180.0 |
| O2−Cu3−O2A | 180.0 | O1−Cu3−O2A | 91.2(2) |

[a] X = a disordered cyanide member atom position.

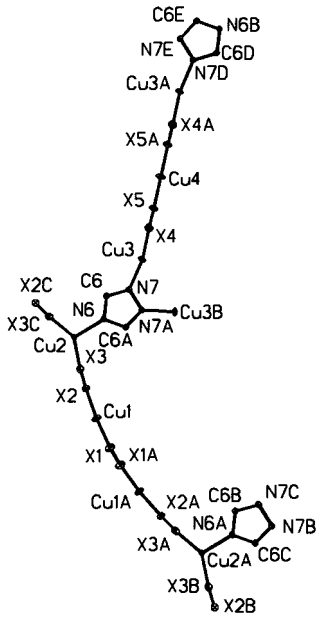


**Figure 1.** A portion of a "slinky" of **1** shown with atoms represented as 50% thermal ellipsoids. Hydrogen atoms are omitted for clarity.

## Results and Discussion

**Syntheses.** The syntheses described for **1**−**5** are analogous to those reported previously by this group for the copper−cyanide−organoamine species $[\{(bpy)Cu\}_2(CN)][Cu_5(CN)_6]$ (**CUNC1**)[16] and $[\{(bpy)Cu\}_2(CN)]_2[Cu_5(CN)_7]\cdot{}^1/_6H_2O$ (**CUNC2**),[17] $[Cu_4(CN)_4(biquin)]$,[16] and $[Cu_3(CN)_3(bipypy)]$.[18] The necessity of including KCN in the syntheses to ensure the growth of single crystals suitable for structural characterization was determined during the earlier preparation of **CUNC1**[16] and **CUNC2**,[17] a practice which was continued here. The only technical variation was the use of borosilicate tubes as opposed to Parr acid digestion bombs. Slightly different charge volumes and solid-phase reagent-to-solvent ratios were employed.

(26) *OMNIC 3.1*; Nicolet Instrument Corp.: Madison, WI, 1992−1996.

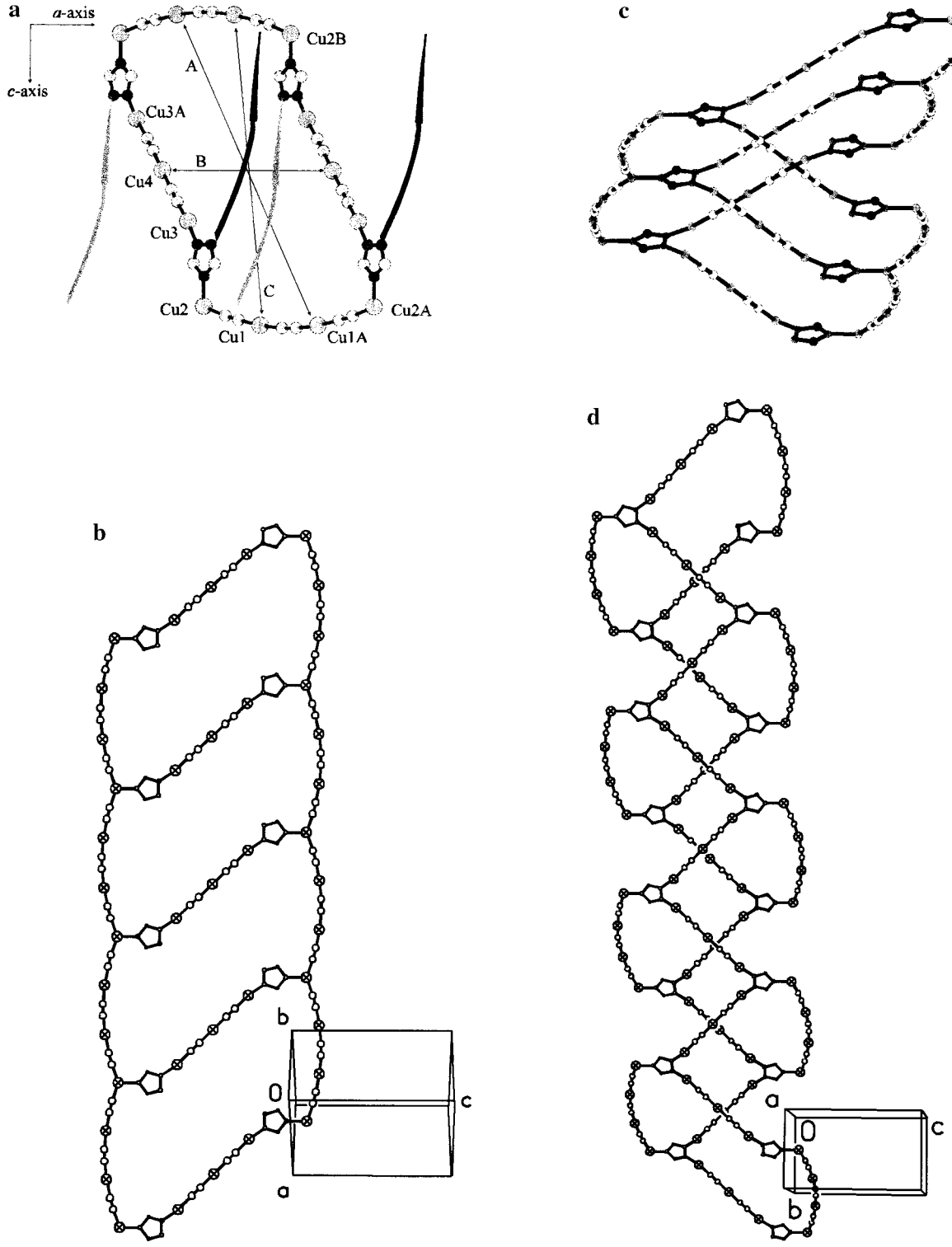


**Figure 2.** (a) A $\{Cu_{14}(CN)_{10}(trz)_4\}$ ring of a "slinky", where light gray arrows and black arrows denote the directions of $\{Cu_3(CN)_2\}$ arms linking adjacent cells of the same "slinky" approaching into and projecting from the ring plane, viewed perpendicular to the *ac* crystallographic plane. Dimensions: $A = 25.5$ Å, $B = 14.2$ Å, $C = 21.4$ Å. Charcoal spheres, large dark gray spheres, small gray spheres, and small light gray spheres represent N, Cu, C, and X atoms, respectively. Hydrogen atoms are omitted for clarity. (b) A ribbon of fused $\{Cu_{14}(CN)_{10}(trz)_4\}$ rings. Hydrogen atoms are omitted for clarity. (c) The intersection of four $\{Cu_{14}(CN)_{10}(trz)_4\}$ rings at a $trz^-$ anion. Charcoal spheres, large dark gray spheres, small gray spheres, and small light gray spheres represent N, Cu, C, and X atoms, respectively. Hydrogen atoms are omitted for clarity. (d) A "slinky" propagating through a layer. Hydrogen atoms are omitted for clarity.

The solid phases obtained directly from hydrothermal media contain copper exclusively in the +1 oxidation state. The thermodynamic stability of Cu(I)−cyanide species with respect to Cu(II) species at elevated temperature and pressure has been commented upon previously.[16−18,27] Only one extended solid-state mixed-valence copper−cyanide compound wherein a Cu(II) site is coordinated directly to a cyanide ligand also bridging to a Cu(I) site has been described.[28] The near

(27) Sharpe, A. G. *The Chemistry of Cyano Complexes of the Transition Metals*; Academic Press: New York, 1976; pp 226−271.
(28) Williams, R. J.; Cromer, D. T.; Larson, A. C. *Acta Crystallogr.* **1971**, *B27*, 1701.

exclusivity of Cu(I) phases may reflect not only the thermodynamic stability of Cu(I) under hydrothermal conditions but also the stabilization of the Cu(I) oxidation state through $\pi$-backbonding to the cyanide and aromatic amine ligands.[29] It is noteworthy that compound **6** was not isolated directly from hydrothermal media but rather crystallized during the evaporation of the mother liquor of **1**.

Deprotonation of the triazole ligand is a common feature of the hydrothermal chemistry of Cu−Htrz systems.[15,30,31] As such, the anionic ligand functions as a tripodal moiety. It is proposed that a shift in p$K_a$ of acidic species under hydrothermal conditions, Htrz in this case, occurs in a manner analogous to that of the shift in p$K_a$ for water,[32] which may preclude the possibility of isolating compounds containing Htrz from Cu−X−Htrz−LL systems.

**Desciptions of the Structures.** The structure of $[Cu_6(CN)_5(trz)]$ (**1**) is composed of neutral interpenetrating layers of flattened, fused "slinkies". The "slinkies" are built from stacked-$\{Cu_x(CN)_y\}$ arms connecting trz anions. The basic components of the structure of **1** are shown in Figure 1, which includes the asymmetric unit. The Cu2 sites of the structure are three-coordinate but distorted from rigorous planarity, with bond angles ranging from ca. 109 to 142°. The Cu1, Cu3, and Cu4 sites are two-coordinate, with Cu4 rigously linear due to crystallographically imposed symmetry. All copper species are formally in an oxidation state of +1, in agreement with the coordination geometries described and charge balance requirements.

The triazole component of **1** is the deprotonated triazolate form, $C_2N_3H_2^-$, ligating in a $\mu_3$ mode to a Cu2 site and to two Cu3 sites. As such, the anionic trz ligands are central to $\{Cu_3(trz)\}$ units of the "slinky" architecture that is the unusual structural motif of **1**.

Two sequential Cu2 sites form the termini of a $\{Cu_4(CN)_3\}$ chain which serves to connect two sequential $trz^-$ ligands, each through an $N^4$ site. A distinct $\{Cu_3(CN)_2\}$ chain with Cu3 and Cu3A termini links the $N^1$ site of a $trz^-$ ligand to the $N^2$ site of the next anionic $trz^-$ ligand in the sequence, as shown in Figure 1. Two chains of each type and four $\mu_3$-bridging $trz^-$ ligands form a 36-member $\{Cu_{14}(CN)_{10}(trz)_4\}$ ring, as shown in Figure 2. The Cu2−Cu2A sequences delimit the height of the cell along the crystallographic *c* axis and consequently the depth of a layer. The nonplanar $\{Cu_{14}(CN)_{10}(trz)_4\}$ ring has dimensions of ca. 25.5 Å × 14.2 Å.

Adjacent rings fuse along the edges containing the Cu3···Cu3A chains to form a ribbon of fused rings propagating parallel to the crystallographic *ab* planes, as shown in Figure 2b. The three-coordinate Cu2 sites serve as the loci for the intersection of infinite $\{Cu(CN)\}_\infty$ chains which delimit the top and bottom of the ribbons and link to the $\{trz-Cu_3(CN)_2-trz\}$ chains which buttress the $\{Cu(CN)\}_\infty$ chains. Alternatively, this ribbon may be described as a ladder structure with the $\{Cu(CN)\}_\infty$ chains forming the side-rails and the $\{trz-Cu_3(CN)_2-trz\}$ chains the rungs.

The layer structure of **1** is constructed by connecting adjacent ribbons through $\{Cu_3(CN)_2\}$ chains linked to the remaining nitrogen donor of each triazolate ligand, as shown in Figure 2c. This connectivity pattern results in each $trz^-$ ligand acting as a pivot to adjacent $\{Cu_{14}(CN)_{10}(trz)_4\}$ rings.

**Chart 2.** A "Slinky" of **1**

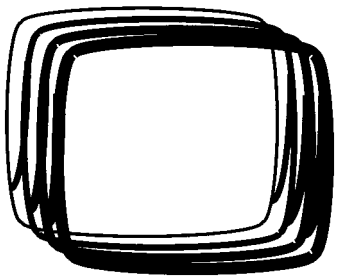

Tracing the path defined by a series of $\{Cu_{14}(CN)_{10}(trz)_4\}$ rings and $\{Cu_3(CN)_2\}$ arms linked through triazolate ligands results in a "slinky" cutting diagonally across the successive ribbons of a layer as shown in Figure 2d and schematically in Chart 2. The structure of **1** is further complicated by interdigitation and interpenetration which serve to fill the potential void volume.

Figure 3a shows four $\{Cu_{14}(CN)_{10}(trz)_4\}$ rings, one from each of four distinct "slinkies". The two rings in the plane of the projection overlap, while the remaining rings interpenetrate to provide a dense space-filling assembly of the layers. When the structure of **1** is viewed parallel to the crystallographic *c* axis, the interpenetration of crystallographically equivalent layers is evident (Figure 3b). Although examples of structures in which two or more independent infinite networks interpenetrate each other were relatively rare until recently, they have been reported with increasing frequency and have been reviewed comprehensively by Batten and Robson.[33] Using their classification scheme, the structure of **1** may be described as an "inclined interpenetrating" two-dimensional network. Interdigitation and interpenetration result in interlayer contacts of ca. 3.3 and 2.7 Å between the Cu sites. The $d^{10}$ closed-shell electronic configuration of Cu(I) species suggests that the interlayer interactions are van der Waals in nature.[34]

The structure of $[Cu_5(CN)_3(trz)_2(bpy)]$ (**2**) is remarkably different from that of compound **1**. The gross structure of **2** can be described as neutral noninterpenetrating corrugated sheets with projecting sidearms. The sidearms of **2** occupy the troughs of adjacent layers.

As shown in Figure 4a, the structure of **2** possesses six unique metal sites. The four metal centers Cu2, Cu3, Cu4, and Cu6 are in distorted trigonal coordination geometries, with bond angles ranging from ca. 103 to 151°. The remaining two sites (Cu1 and Cu5) are in linear coordination geometries. The Cu1 sites which bond to two cyano units provide the midpoint of $\{Cu_3(CN)_2\}$ chains. The three-coordinate Cu2 sites are the termini of these $\{Cu_3(CN)_2\}$ chains and are also coordinated to one of the $\mu_3$-trz ligands which serve to bond to two other three-coordinate metal sites, Cu3 and Cu4. The cyano unit coordinated to the Cu4 site bridges to the Cu6 site whose coordination is completed by a chelating bpy ligand.

The $\{Cu_3(trz)\}$ units are the components of the fundamental $\{Cu_4(trz)_2\}$ building block (Chart 3) of **2**. The $\{Cu_2N_4\}$ ring formed by the endo Cu atoms and the 1- and 2-nitrogen donors of the trz ligands (Chart 3) is not planar. The Cu4 site of the $\{Cu_2N_4\}$ ring serves as the anchor for the {(CN)Cu(bpy)} sidearm, with the {Cu4(CN) vector inclined at ca. 26° with respect to the$\{Cu_2N_4\}$ least-squares plane.

As shown in Figure 4a and 4b, the Cu3 and Cu4 centers are bridged by two $trz^-$ ligands, the second of which bonds to the

(29) Cooper, D.; Plane, R. A. *Inorg. Chem.* **1996**, *5*, 2209.
(30) Zapf, P. J.; Zubieta, J. Unpublished results.
(31) Hammond, R. P.; Zubieta, J. Unpublished results.
(32) Sweeton, F. H.; Mesmer, R. E.; Baes, C. F., Jr. *J. Solution Chem.* **1974** *3*, 191.
(33) Batten, S. R.; Robson, R. *Angew. Chem., Int. Ed. Engl.* **1998**, *37*, 1460−1494.
(34) Pykkö, P.; Runeberg, N.; Fernando, M. *Chem.—Eur. J.* **1997** *3*, 1451.

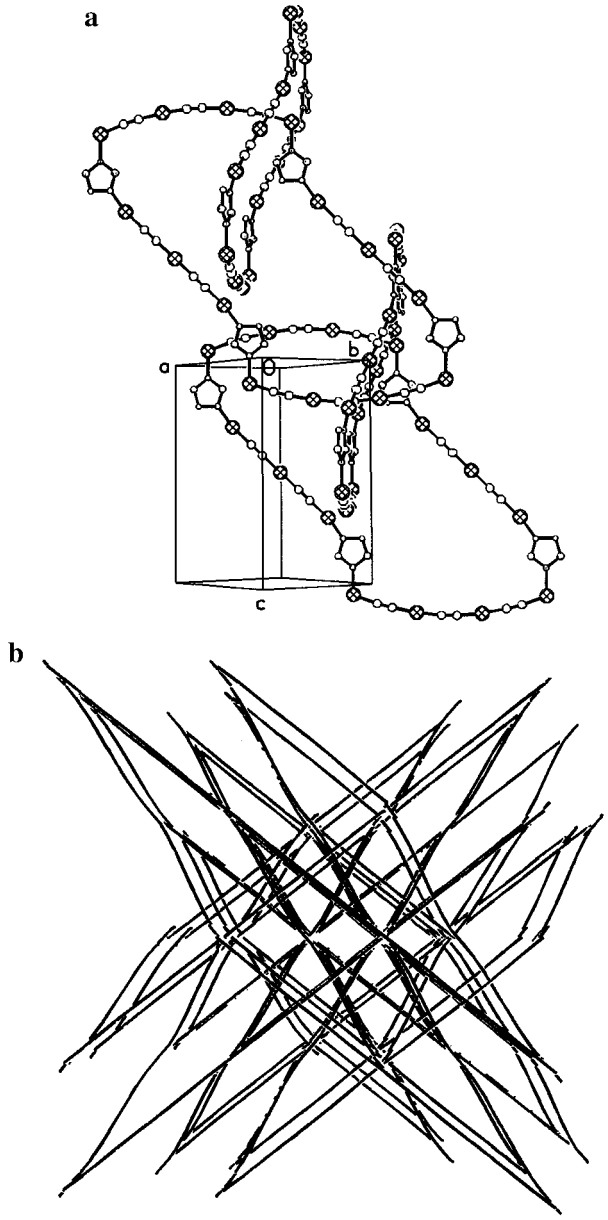


**Figure 3.** (a) Interpenetration and interdigitation of four $\{Cu_{14}(CN)_{10}(trz)_4\}$ rings that compose "slinkies" that form four distinct layers. Each ring is from a different "slinky". Hydrogen atoms are omitted for clarity. (b) Line representation of the crystal structure of **1** viewed perpendicular to the *ab* crystallographic plane.

two-coordinate Cu5 center through the $N^4$ site. The third ligands of the Cu3 and Cu4 centers are cyanide groups.

The Cu5 site acts as a tether for two adjacent $\{Cu_4(trz)_2\}$ units in forming a "two-block" unit. Adjacent "two-block" units are linked in turn by cyanide ligands bonding to the Cu2 and Cu3 sites to produce a staggered rope ladder motif (Figure 4b, Chart 4) when viewed perpendicular to the crystallographic *ac* plane, with the "two-block" units acting as the rungs of the ladder while the cyanide ligands constitute the linking ropes. Large rings, $\{Cu_8(CN)_2(trz)_6\}$ (A), of approximate dimensions 17.3 Å × 4.6 Å (not accounting for hydrogen atoms) are formed by fusing two "two-block" units through two cyanide linkages.

Short $\{Cu_3(CN)_2\}$ chains link adjacent ladders to form a corrugated layer with rows of $\{Cu_8(CN)_6(trz)_2\}$ rings (B) which alternate with the ladders of rings A in the layer structure. Adjacent B rings have the $\{Cu_3(CN)_2\}$ ties as their common edge and have approximate dimensions of 15.7 Å × 9.1 Å.

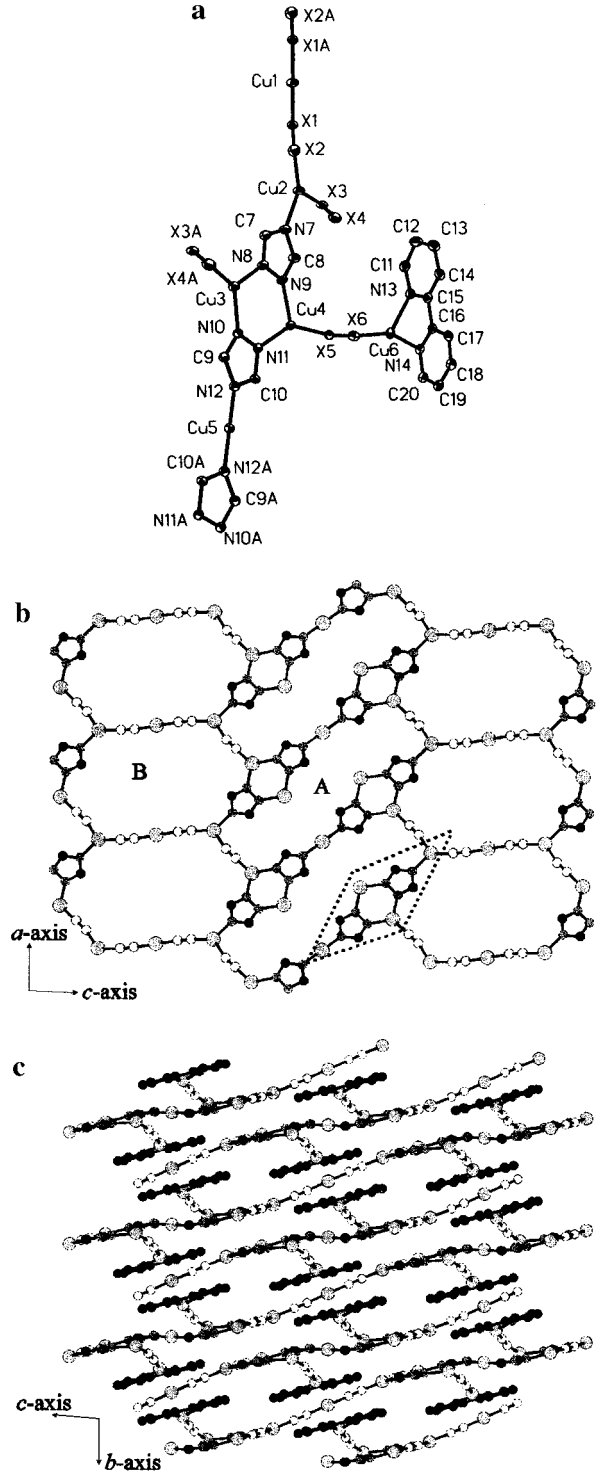


**Figure 4.** (a) View of the metal coordination sites of **2**, showing the atom labeling and 50% thermal ellipsoids. Hydrogen atoms are omitted for clarity. (b) View of the layer of **2**. The {(CN)Cu(bpy)} pendant groups are omitted for clarity as are hydrogen atoms. The dashed rhombus outlines the $\{Cu_4(trz)_2\}$ building block. An A and a B ring are defined. Black, large dark gray, small dark gray, and small light gray spheres represent C, Cu, N, and X postitions, respectively. (c) View of **2** perpendicular to the crystallographic *bc* plane. Hydrogen atoms are omitted for clarity. Black, large dark gray, small dark gray, and small light gray spheres represent C, Cu, N, and X positions, respectively.

The {(CN)Cu(bpy)} sidearms projecting from the layer are composed of {(CN)Cu} tethers and bpy caps with the least-squares plane of the bpy ligands nearly parallel to the vicinal plane of the parent layer and to the plane of the adjacent layer

**Chart 3**

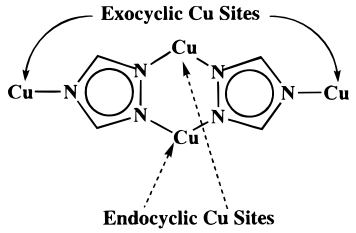


**Chart 4.** Structural Motifs of Compounds **2**−**5**

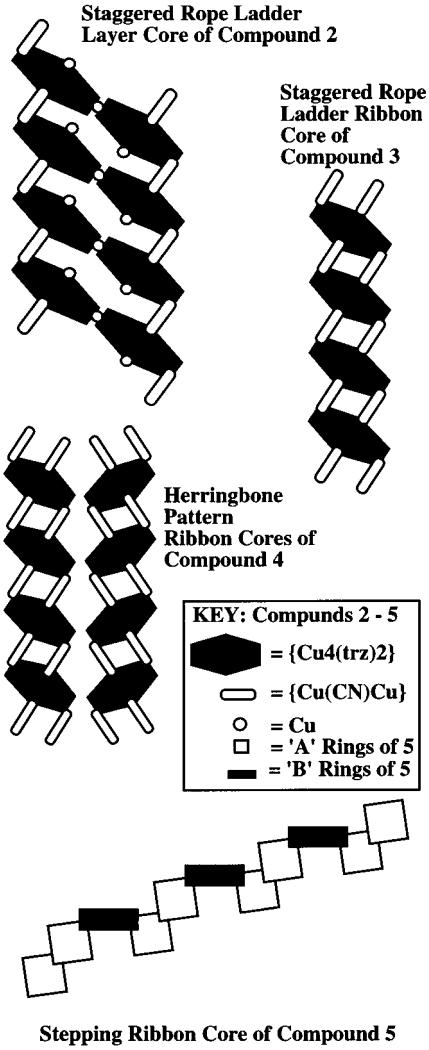


(Figure 4c). The plane of the bpy ligand is inclined ca. 23.4° to the sidearm metal−cyanide tether axis. Interestingly, the sidearms exhibit conformations similar to those described for the $\{(bpyCu)_2(CN)\}^+$ cations of the compounds **CUNC1**[16] and **CUNC2**[17] reported previously. Attached to each "two-block" unit are two {(CN)Cu(bpy)} pendant groups, one disposed above and one below the layer. The bpy ligands are located proximal to the Cu5 site across the large ring A from the parent anchor site but are not coplanar with this ring, as shown in Figure 4a,c.

Compound **3**, $[Cu_3(CN)_2(trz)(bpy)]$, is a neutral one-dimensional ribbon with some similarities to the structure of compound **2**. The structure of **3** contains three unique Cu(I) sites in distorted trigonal coordination geometries as shown in Figure 5a.

The structure of **3** exhibits the $\{Cu_4(trz)_2\}$ building blocks previously observed for **2** (Chart 3). The Cu1 site forms part of

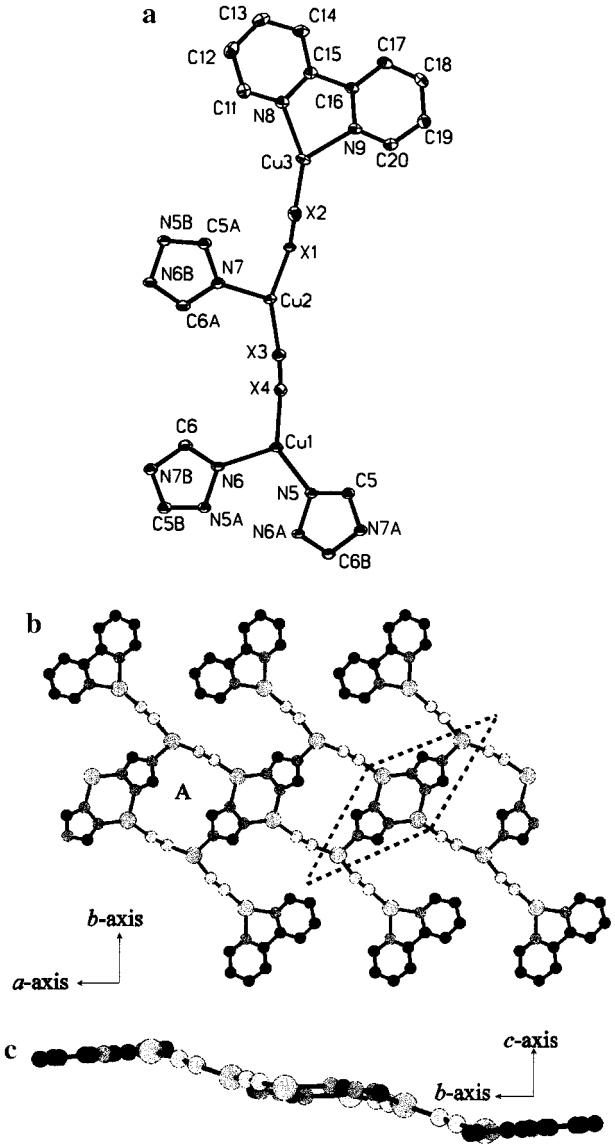


**Figure 5.** (a) Coordination geometries of the metal centers of **3**, showing the atom-labeling scheme and 50% thermal ellipsoids. Hydrogen atoms are omitted for clarity. Symmetry equivalents of C5, C6, N5, N6, and N7 are included. (b) View of the ribbon of **3** perpendicular to the crystallographic *ab* plane. The dashed rhombus outlines the $\{Cu_4(trz)_2\}$ building block. Black, large gray, small dark gray, and small light gray spheres represent C, Cu, N, and X atoms, respectively. An A ring is denoted. Hydrogen atoms are omitted for clarity. (c) Rippling of the ribbon cross section of **3**. The view is parallel to the crystallographic *a* axis. Hydrogen atoms are omitted for clarity.

the $\{Cu_2N_4\}$ core of this unit and additionally bonds to a cyanide ligand bridging to the Cu2 site, which is also the exocyclic metal center of the $\{Cu_4(trz)_2\}$ units. The coordination about Cu2 is completed by a cyanide bridge to the Cu3 center which in turn bonds to a bpy chelate.

The ribbon structure of compound **3**, as shown in Figure 5b, is constructed from the $\{Cu_4(trz)_2\}$ blocks linked by cyanide bridges at the four endocyclic to exocyclic Cu sites of the adjacent blocks, so as to form $\{Cu_4(CN)_2(trz)_2\}$ rings, A, having dimensions 7.9 Å × 4.6 Å and propagating parallel to the crystallographic *a* axis. A staggered rope ladder results (Chart 4).

The Cu3 sites participate in {(CN)Cu(bpy)} sidearms, similar to the unit previously described for **2**, which project from the central ribbon and which are anchored at the Cu2 sites. The

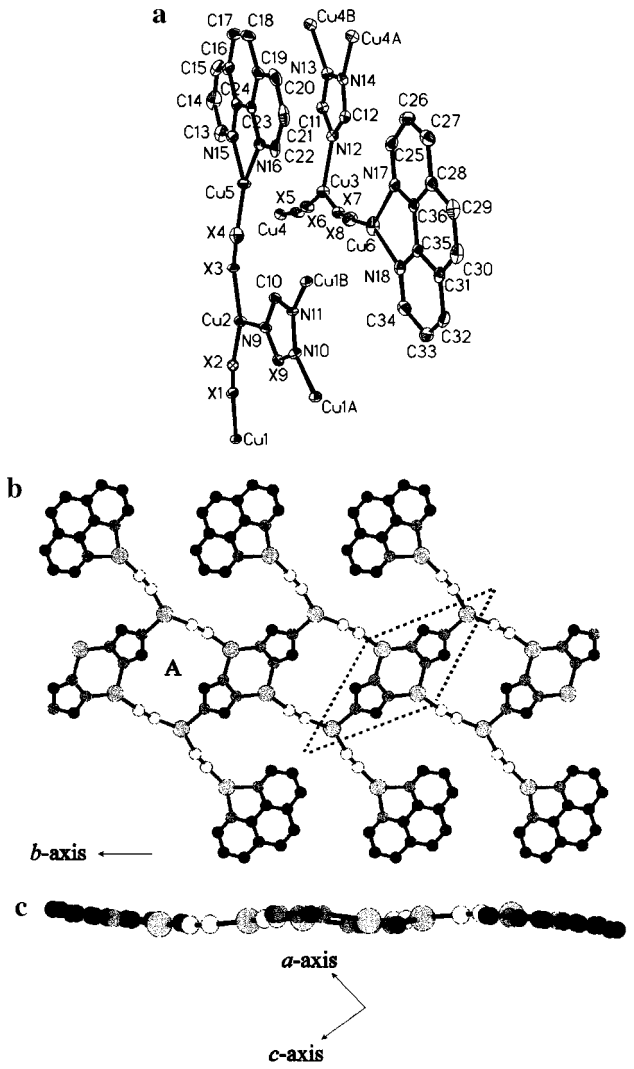


**Figure 6.** (a) Coordination geometry of the metal sites of **4**, showing the atom-labeling schemes and 50% thermal ellipsoids. Hydrogen atoms are omitted for clarity. (b) View of the ribbon structure of **4**. The dashed rhombus represents the $\{Cu_4(trz)_2\}$ building blocks. An A ring is defined. Black spheres, large gray spheres, small dark gray spheres, and small light gray spheres represent C, Cu, N, and X atoms, respectively. Hydrogen atoms are omitted for clarity. (c) Cross section of a ribbon of **4** shown perpendicular to the crystallographic *ac* plane. Black spheres, large gray spheres, small dark gray spheres, and small light gray spheres represent C, Cu, N, and X atoms, respectively. Hydrogen atoms are omitted for clarity.

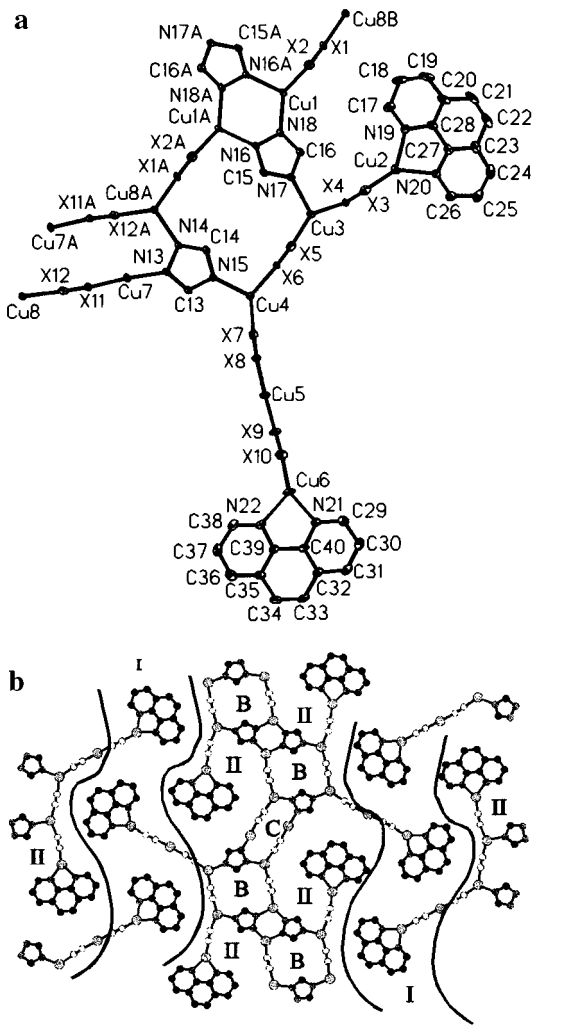


**Figure 7.** (a) View of the metal coordination geometries of **5**, showing the atom-labeling scheme and 50% thermal ellipsoids. Hydrogen atoms are omitted for clarity. (b) View of the fragments of three ribbons of **5**. B and C rings are defined. Type I and type II pendant groups and the domains formed by them are indicated by thick black lines. Black spheres, large gray spheres, small dark gray spheres, and small light gray spheres represent C, Cu, N, and X atoms, respectively. Hydrogen atoms are omitted for clarity.

{Cu(CN)} tether of the sidearm makes an angle of ca. 17.5° with the bpy plane. The cant of the sidearm tether and the bpy components give the ribbon a rippled, not planar, appearance when viewed in cross section parallel to the crystallographic *a* axis as shown in Figure 5c.

The material $[Cu_3(CN)_2(trz)(phen)]$ (**4**) is constructed from building blocks similar to those described for **3**. Once again, $\{Cu_4(trz)_2\}$ blocks are linked through cyanide bridges to form a central rope ladder motif, as shown in Figure 6a,b. The A-type rings $\{Cu_4(CN)_2(trz)_2\}$ which are formed by this connectivity pattern have approximate dimensions 8.0 Å × 4.6 Å. The Cu2 sites again provide an anchor for the pendant side chains, in this instance{(CN)Cu(phen)} groups.

Ribbons of the same relative orientation of the $\{Cu_4(trz)_2\}$ blocks are aligned in layers. Ribbons in adjacent layers are aligned in the opposite sense, such that a herringbone pattern is observed when ribbons from consecutive layers are viewed perpendicular to the ribbon planes as shown in Chart 4.

The ribbons of **4** approach planarity more closely than those of **3**, as shown in Figure 5c. The {Cu(CN)} tethers of the sidearms of **4** make an angle ca. 10.8° with the phen planes, compared to an angle of 17.5° for the {Cu(CN)} linkages of **3** to the bpy planes.

Compound **5**, $[Cu_4(CN)_3(trz)(phen)]$, also forms a neutral one-dimensional ribbon. As shown in Figure 7a, the structure is constructed from eight crystallographically unique copper centers. Copper atoms Cu5 and Cu7 exhibit digonal coordination, while all others are in distorted trigonal environments. The Cu1 and Cu3 sites participate in the construction of the $\{Cu_4(trz)_2\}$ blocks, common to the structures of **2**−**5**. However, in contrast to structures **3** and **4**, these blocks are not directly linked through cyanides to form A-type rings as in **3** and **4** but are joined through cyanide bridges to secondary $\{Cu_3(trz)\}$ moieties, so as to form $\{Cu_2(CN)_2(trz)_2\}$ rings B.

The $trz^-$ ligands of these $\{Cu_3(trz)\}$ groups connect the Cu4, Cu7, and Cu8 sites. Cyanide bridging ligands from Cu7 and Cu8 connect adjacent B rings and form an additional building block, the $\{Cu_2(CN)_2(trz)_2\}$ ring C. The consequence of this connectivity pattern is ribbons with a BBCBBC repeat pattern

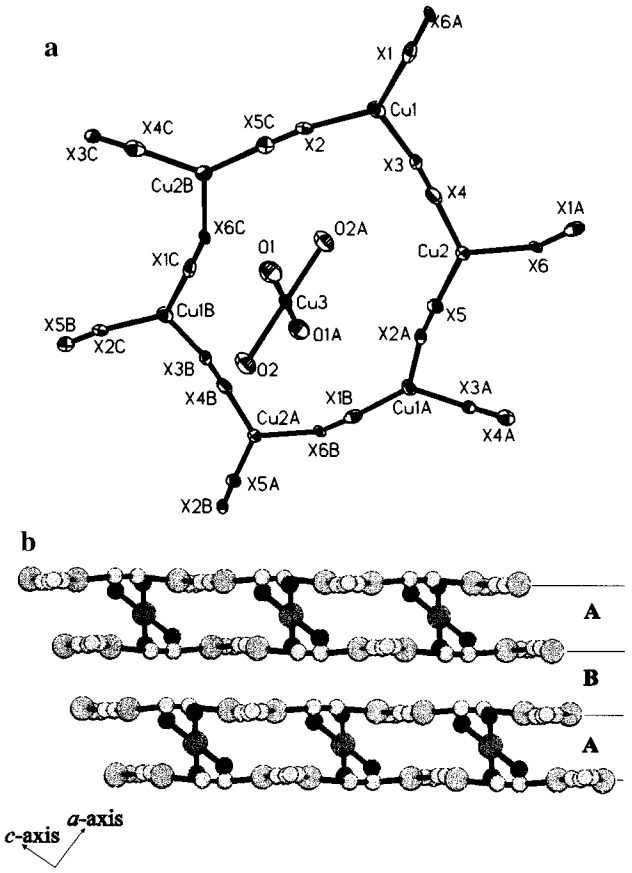


**Figure 8.** (a) A $\{Cu_6(CN)_6\}$ ring and $\{Cu(OH_2)_4\}^{2+}$ cation of **6** with 50% thermal ellipsoids. Hydrogen atoms are omitted for clarity. (b) View of **6** shown perpendicular to the crystallographic *ac* plane. The AB stacking of the layers and inclination of the cations to the copper−cyanide layers is shown. Dark gray spheres, large light gray spheres, and small light gray spheres represent O, Cu, and X atoms, respectively. Hydrogen atoms are omitted for clarity.

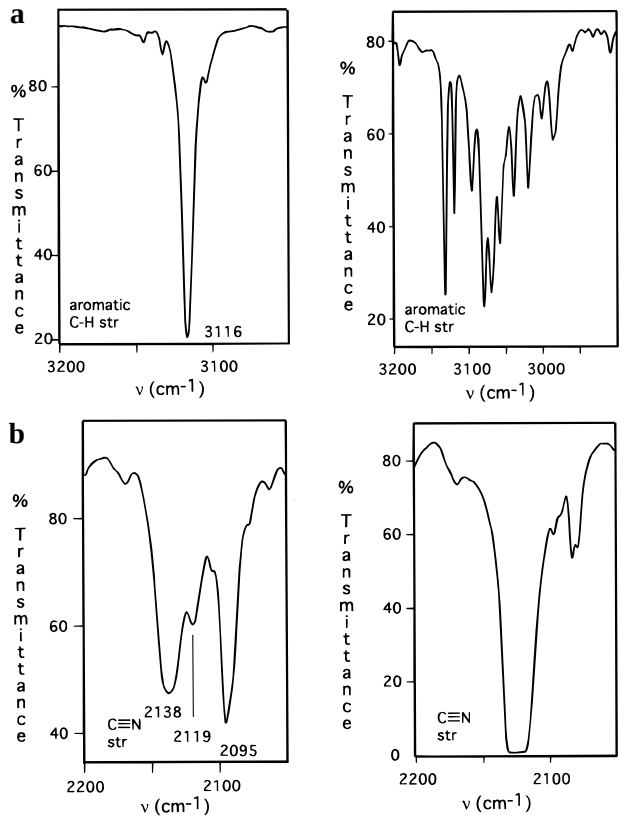


**Figure 9.** (a) C−H and cyanide stretching regions of **1**. (b) C−H and cyanide stretching regions of **2**.

of rings, as shown in Figure 7b. When viewed schematically (Chart 4), the structure appears as a stepped ribbon.

The structure of **5** is further distinguished by the presence of two distinct pendant groups. The type I groups $\{Cu_2(CN)_2(phen)\}$, which anchor to the Cu4 sites, are oriented with the $\{Cu_2(CN)_2\}$ tether axes approximately perpendicular to the stepped ribbon axis of propagation which is parallel to the crystallographic *b* axis. Type I groups from adjacent ribbons interdigitate to generate a domain of side to side oriented phen groups. The {(CN)Cu(phen} type II groups project from Cu3 sites to lie nearly parallel to the axis of propagation of the ribbon core. The individual phen components of the type II sidearms are isolated from each other by the ribbon core, the $\{Cu_2(CN)_2\}$ tethers of the type I sidearms, and the domain of phen molecules described above (Figure 7b). The phen planes are inclined at ca. 5.5 and 5.8° to $\{Cu(CN)\}_n$ tether axes, respectively.

The structure of compound **6**, $[Cu(OH_2)_4]\{Cu_4(CN)_6\}$, consists of $\{Cu_4(CN)_6\}_n^{2n-}$ anionic layers intercalated by $\{Cu(OH_2)_4\}$ dications in alternate interlammellar spaces. Charge balance requirements dictate that the Cu sites in the layers are all in the +1 oxidation state, an observation confirmed by the geometries of those sites. The tetracoordinate Cu atom of the tetraaquacupric dication assumes the +2 oxidation state as required by charge balance and metrical parameters (Figure 8a).

The layer structure of **6** is constructed from distorted trigonal planar Cu centers linked into 18-member $\{Cu_6(CN)_6\}$ rings of dimensions 11.7 Å × 6.8 Å, which fuse into a distorted honeycomb (Figure 8a). The 18-member $\{Cu_6(CN)_6\}$ rings of compound **6** are not analogous to the rings of the same formulation contained in the layered species **CUNC2**,[17] which was isolated directly from hydrothermal media. The 18-member rings of the structure of compound **6** are not, however, completely analogous to the $\{Cu_6(CN)_6\}$ rings of $[KCu_2(CN)_3]\cdot H_2O$.[35]

The $\{Cu(OH_2)_4\}^{2+}$ cations occupy the interlamellar space inclined at an angle of 53° with respect to the layer least-squares plane and align with the ring cavities of the layers. The intercalation of the tetraaquacupric dications in alternate interlamellar spaces results in an ABAB repeat pattern for the layers of **6**, with interlamellar spacings of 3.4 and 3.1 Å rings for A and B, respectively, as shown in Figure 8b.

**FTIR Spectroscopy.** The spectrum of **1** (Figure 9a) exhibits a characteristic band at 3116 $cm^{-1}$ associated with $\nu$(C−H) of the triazolate ligand. The cyanide stretching region of the spectrum of **1** was somewhat complex with peaks appearing at 2138, 2119, and 2095 $cm^{-1}$, an observation consistent with the inequivalence of the cyanide sites of **1**.

The aromatic $\nu$(C−H) regions for compounds **2**−**5** were more complicated than that of **1** as anticipated from the presence of the aromatic organoamines bpy and phen. These aromatic features appear in the 3200−2900 $cm^{-1}$ region for **2**−**5**.

In contrast to the $\nu$(CN) pattern observed for **1**, compounds **2**−**5** exhibited strong broad bands centered at ca. 2125 $cm^{-1}$ and weak bands at ca. 2190 $cm^{-1}$ (Figure 9b). It is noteworthy that **1** is the only member of this class of materials to exhibit $\{Cu(CN)\}_\infty$ chains, suggesting that the unique CN stretching region of its spectrum reflects the presence of this structural feature.

(35) Cromer, D. T.; Larson, A. C. *Acta Crystallogr.* **1962**, *15*, 397.

**Summary of the Structures.** As anticipated, the bridging ability of the cyanide and triazolate ligands favor the propagation of structural motifs in the construction of extended structures. Since the triazolate ligand is in the deprotonated form under the conditions of the experiments, it appears exclusively in the $\mu_3$-bridging mode. Consequently, the $\{Cu_3(trz)\}$ unit is a ubiquitous component in **1**−**5** and other solid-state materials formed under hyrothermal conditions.[30,31] The $\{Cu_3(trz)\}$ unit is proposed as a progenitor from which all solid-state materials of hydrothermal origin in the Cu−trz family subsequently evolve. The versatility of the connectivity motifs linking these $\{Cu_3(trz)\}$ units provides in the rich structural chemistry summarized in Charts 2 and 4.

It is also apparent that the $\{Cu_3(trz)\}$ units fuse to provide the $\{Cu_4(trz)_2\}$ cluster which provides a fundamental building block for the structures of **2**−**5**. That such a $\{M_4(trz)_2\}$ unit may be generic to a variety of chemical families is suggested by the structure of [Zn(trz)Cl].[36] Furthermore, it is noteworthy that chelating nitrogen donor ligands serve to terminate the propagation of the structure perpendicular to the chain axis, thus serving in a passivating role by blocking metal coordination sites. The role of such ligands is in contrast to the templating or simple space-filling functions generally associated with organic components. However, secondary space-filling roles are not excluded as indicated by the structure of **5**, where the type I pendant groups of the ribbon appear to constrain the orientation of the type II pendants.

The deviation from planarity of the {Cu(CN)(LL)} units of the structures are similar to but not as extensive as those previously reported for **CUNC1** and **CUNC2**.[16,17] Such distortions reflect crystal packing forces, and nearly planar conformations are observed when packing permits, as in **5** and $[Cu_4(CN)_4(biquin)]$.[16]

Interestingly, no triazolate- or triazole-containing compounds were isolated from hydrothermal media when biquin and bipypy were reactants.

## Conclusion

A series of novel and complex structure types of the copper−cyanide−organoamine family have been isolated from hydrothermal media and structurally characterized. The results reinforce the observation that hydrothermal chemistry offers an effective synthetic tool for the isolation of composite organic−inorganic materials. It is also clear that organic ligands with specific geometric requirements may be introduced as structural components of materials. Bridging ligands may be used to propagate the architecture about a metal site, while chelating agents may serve to passivate the metal coordination sphere so as to limit the spatial extension of the material. Manipulation of the microstructure of the solid is thus achieved by tuning the coordination influences of the metal to the geometric requirements of the ligand.

The anionic ligands cyanide and 1,2,4-triazolate are ideal species for bridging metal centers and propagating a variety of structural motifs in the construction of extended solids. In contrast, chelating agents may serve in terminating roles, restricting the spatial extensions of the material. A secondary space-filling role is also adopted by these ligands.

While it is now evident that organic components may be introduced into the synthesis of solid-state inorganic materials to manipulate the coordination chemistry of the metal and consequently the structure of the material, designed extended structures remain elusive in the sense of predictability of the structure. However, this observation reflects the compositional and structural versatility of inorganic materials and should be considered an opportunity for development rather than an occasion for lamentation. The subtle interplay of metal oxidation states, coordination preferences, polyhedral variability, ligand donor groups, types, and orientations, spatial extension, and steric constraints provides a limitless set of construction components for solid-state materials. As the products of empirical observations are elucidated, the structure−function relationships of such components will begin to emerge and to provide further guidelines for synthetic methodologies.

**Acknowledgment.** We thank P. J. Zapf and R. P. Hammond for insightful comments regarding the structures of the triazolate-containing compounds. Funding for this work was provided through NSF Grant CHE9617232, NIH Grant GM34548, and the W. M. Keck Foundation.

**Supporting Information Available:** Listings of crystal data and collection parameters, atomic positional parameters, anisotropic thermal parameters, and all bond lengths and angles for **1**−**6**. This material is available free of charge via the Internet at http://pubs.acs.org.

IC990385Q

(36) Kröber, J.; Bkouche-Waksman, I.; Pascard, C.; Thoman, M.; Kahn, O. *Inorg. Chim. Acta* **1995**, *230*, 159.